引用格式:NIU Qi-qiang, HUO Yi-ping, JIANG Xue-ying, *et al*. Multiple Magnetic Fano Resonances Based on Single-split Ring and Double-split Disk Structure[J]. *Acta Photonica Sinica*, 2019, **48**(9):0926001
牛启强,霍义萍,姜雪莹,等. 基于单劈裂环-双劈裂盘结构的多重磁 Fano 共振[J].光子学报,2019,**48**(9):0926001

基于单劈裂环-双劈裂盘结构的多重磁 Fano 共振

牛启强,霍义萍,姜雪莹,周辰,郭懿圆,侯艺博,何倩,郝祥祥
(陕西师范大学 物理学与信息技术学院,西安 710062)

摘 要:采用有限元方法对单劈裂环-双劈裂盘纳米结构的表面等离激元共振进行了理论研究.当入射光垂直于结构表面时,亮磁模式和暗磁模式相互干涉会产生磁 Fano 共振.当双劈裂盘、空腔和单劈裂环的间隙同时沿 x 轴负方向偏移时,可产生高阶磁模式和双重磁 Fano 共振.在此结构的基础上,进一步调节单劈裂环的间隙宽度,可以在近红外区域增强磁模式的强度,并产生三重磁 Fano 共振;同样地,通过调节双劈裂盘的上劈裂角,在可见光区域可得到新的高阶磁模式,并产生三重磁 Fano 共振.此外,该结构的最大灵敏度和磁场增强分别达到 1 400 nm/RIU 和 69.7 倍.这些光学特性使得该结构在超灵敏度生物传感器和多控磁 Fano 开关领域具有潜在的应用价值.

关键词:表面等离激元;有限元分析;高阶磁模式;多重磁 Fano 共振;折射率灵敏度
中图分类号:O436 **文献标识码**:A **doi**:10.3788/gzxb20204909.0926001

Multiple Magnetic Fano Resonances Based on Single-split Ring and Double-split Disk Structure

NIU Qi-qiang, HUO Yi-ping, JIANG Xue-ying, ZHOU Chen, GUO Yi-yuan, HOU Yi-bo, HE Qian, HAO Xiang-xiang
(*School of Physics and Information Technology, Shaanxi Normal University, Xi'an* 710062, *China*)

Abstract: The surface plasmon resonances of a nanostructure composed of a single-split ring and a double-split disk is studied theoretically by the finite element method. When the incident light is normal to the structure surface, a magnetic Fano resonance can be generated by the interference between a bright magnetic mode and a dark magnetic mode. High order magnetic modes and double magnetic Fano resonances can be generated when the double-split disk, the cavity, and the gap of the single-split ring offset together along the negative x-axis. On the basis of this structure, further modulating the gap width of the single-split ring, magnetic modes intensity is enhanced in the near-infrared region and triple magnetic Fano resonances is generated; similarly, by modulating the upper split angle of the double-split disk, high-order magnetic mode is obtained in the visible region and triple magnetic Fano resonances is generated. In addition, the maximum sensitivity and magnetic field enhancement of the structure can reach 1 400 nm/RIU and 69.7, respectively. These optical properties make the structure has potential application value in the field of ultra-sensitive biosensor and multi-control magnetic Fano switch.

Key words: Surface plasmons; Finite element method; High order magnetic modes; Multiple magnetic Fano resonances; Refractive index sensitivity
OCIS Codes: 260.3160; 260.3910; 260.5740; 240.6680; 250.5403

Foundation item: National Natural Science Foundation of China (No.11604198)
First author: NIU Qi-qiang (1995—), male, M.S. degree candidate, mainly focuses on surface plasmon. Email: 1943560720@qq.com
Supervisor (Contact author): HUO Yi-ping (1977—), female, associate professor. Ph.D. degree, mainly focuses on surface plasmon and micro-nano optics. Email: yphuo@snnu.edu.cn
Received: Apr.24, 2020; **Accepted**: Jul.8, 2020

0 Introduction

Surface Plasmons (SPs) is an electromagnetic wave formed by the interaction of free electrons and photons in a metal surface region[1-3]. It is able to break through the traditional optical diffraction limits and has a strong local field enhancement. SPs is very sensitive to the shape and size of the structure, the refractive index of the environment and the polarization direction of the excitation light[4-6]. These properties are of great significance for spectral regulation. For Fano resonance in the SPs system, the radiation attenuation is effectively suppressed. The energy of incident light field can be better localized on the surface of metal nanostructure, thus obtaining more fine spectrum and larger local electric field enhancement[7-8]. These characteristics make Fano resonance have a huge application prospect in biosensing[9-10], surface enhanced Raman spectroscopy and micro-nano optics[11-12].

Fano resonance can be generated by the interference between a bright mode (superradiant) and a dark mode (subradiant). The bright mode has a large net dipole moment, which has a large radiation damping and a wide linewidth in the spectrum. The bright mode can be excited by incident light directly. The net mode dipole moment of the dark mode is almost zero, so it has a small radiation damping and presents a narrower linewidth in the spectrum[13]. The dark mode can't be excited by incident light directly, which can be excited by near-field coupling or symmetry breaking[14]. The Fano resonance line type is asymmetric and sharp[15], which is very sensitive to the change of external environment refractive index and structural parameters. Because of these characteristic, Fano resonance has potential application value in the field of high sensitivity sensors[16]. Single Fano resonance has been studied extensively. At present, multiple Fano resonances received much attention for it can modulate spectrum at multiple wavebands. KHAN A D et al. reported multiple Fano-like resonances are induced by the interference between bright and dark plasmon modes in three-layered bimetallic nanoshell dimer[17]. In addition, KHAN A D's team also investigated multiple plasmonic Fano resonances, which can be induced by the modes coupling based on the split nano-ring structure[18]. LIU Shao-ding et al. demonstrated multiple Fano resonances can be achieved in the plasmonic heptamer clusters, which can be switched on and off by adjusting the polarization direction[19]. LI Jing et al. reported multiple Fano resonances and the dark multiple modes are excited in the two ring/disk cavities nanostructure[20].

The study of magnetic mode originated from its critical role in the study of negative refractive materials[21-23]. Magnetic mode can be applied to sensors, artificial magnetism and magnetic plasma waveguide[24-26]. However, the "magnetic saturation" of natural materials hinders the realization of magnetic mode[27]. In fact, magnetic Fano resonance can be generated by the inducted displacement current loop in the SPs system. Therefore, the displacement current loop is critical to the generation of magnetic Fano resonance[28-32]. Many structures have been designed to study magnetic Fano resonance, such as dielectric polymer, metal polymer, metal and dielectric composite structure[31, 33-35]. SHSFIEI F et al. demonstrated magnetic Fano resonance is induced by the strong magnetic and electric responses in a subwavelength plasmonic metamolecule consisting of four closely spaced gold nanoparticles[28]. BAO Yan-jun et al. investigated a purely magnetic Fano resonance which can be realized at optical frequency with Au split ring hexamer nanostructure with an azimuthally polarized incident light[34]. CHERQUI C et al. reported all-magnetic Fano can be induced by the interference between the bright and dark magnetic modes based on plasmon oligomer dimers[32]. The radiation loss of magnetic Fano resonance is small, which can be applied to negative refractive index metamaterials and low loss magnetic surface plasmon waveguide[36-37]. Although many structures about multiple Fano resonances have been proposed, the design of a novel structure that can generate and regulate multiple magnetic Fano resonances is still a research hotspot.

In this paper, a nanostructure consisting of a Single-split Ring and a Double-split Disk (SSR-DSD) is designed and studied. Magnetic modes and magnetic Fano resonance are excited when the structure surface is illuminated by the plane electromagnetic wave. High order magnetic modes and multiple magnetic Fano resonances can be generated when the double-split disk, the cavity and the gap of the single-split ring offset together along the negative x-axis. On the basis of the structure with offset, magnetic modes and

magnetic Fano resonance can also be generated in the near-infrared and visible wavelengths by modulating the gap width of the single-split ring and the upper split angle of the double-split disk. At the same time, the maximum sensitivity (S) and Figure of Merit (FOM) of the structure can reach 1 400 nm/RIU and 29.43, respectively[38-39]. The maximum electric and magnetic field enhancement of the structure are 290.8 and 69.7, respectively. The structure has potential application in ultra-sensitive biosensor and multi-control magnetic Fano switch.

1 Structure model and simulation method

The schematic of the SSR-DSD nanostructure is shown in Fig.1. The centers of the single-split ring and double-split disk are O and O_1, respectively. R, w and g are the outer radius, width and gap width of the single-split ring. R_1 and θ are the radius and the split angle of the double-split disk. The thickness of the structure is T. The parameters of the structure are $R=100$ nm, $R_1=70$ nm, $w=30$ nm, $T=40$ nm, $g=10$ nm and $\theta=10°$, respectively. The pure metal nanostructure is the free-standing and aperiodic structure.

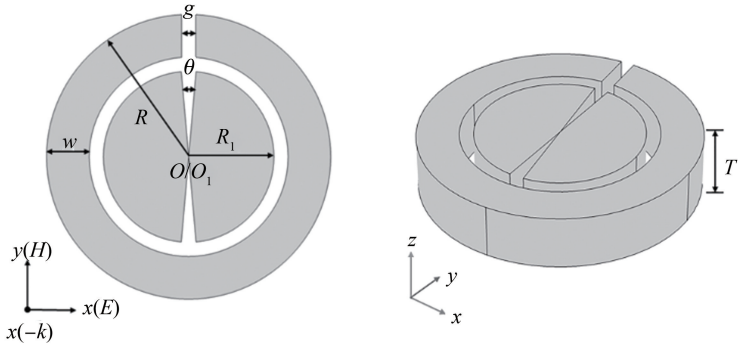

(a) 2-D graph of the SSR-DSD nanostructure (b) 3-D graph of the SSR-DSD

Fig.1 Schematic of the SSR-DSD nanostructure

In the article, silver (Ag) is chosen as the material of metallic elements because it has the low loss properties[1]. The refractive index data of silver used in our numerical simulation are obtained from Johnson and Christy (JC)[40]. An plane electromagnetic wave incidents along negative z-direction and polarizes along x-axis. The Comsol Multiphysics is used to do all the calculations, which is a multiphysics simulation software based on the finite element method[41]. The structure is surrounded by a dielectric layer, which is air. In order to eliminate the influence of electromagnetic wave reflection on the boundary, a perfect matching layer is placed outside the air layer. We mainly study the extinction cross section of the SSR-DSD structure, which is defined as the sum of the scattering cross section and the absorption cross section. The scattering cross section is the amount of scattering energy flow through the entire closed outer surface of the nanostructure. Energy loss in a nanostructure is defined as the absorption cross section[42].

2 Results and discussion

2.1 The spectral properties of the SSR-DSD nanostructure

Fig.2(a) shows the extinction cross section of the SSR-DSD nanostructure. There are four peaks and two dips in the spectrum when the structure surface is illuminated by the plane electromagnetic wave. From left to right, the resonance peaks are named M_1, M_2, M_3, M_4, and the dips are named m_1 and m_2. To further explore the mechanism of these peaks and dips. Fig.2(b)~(i) show the charge distributions, the current density and magnetic field enhancement distributions of mode M_1, M_2, M_3 and dip m_2. The red and blue colors represent the positive and negative charge, respectively. The color bars represent the amplitude of $|H|/|H_0|$, here H represents the local magnetic field, and H_0 represents the background magnetic field. As shown in Fig.2(b), M_1 is an octupole-hexadecapole mode, which is a dark mode. In Fig. 2(f), M_1 has two magnetic hot spots and two opposite current loops, so M_1 is a high-order dark magnetic mode. Fig.2(c) shows that mode M_2 is a quadrupole-octupole mode. According to the charge distribution, the net dipole moment of mode M_2 is almost zero and the line width is narrow, so M_2 is a dark mode. A

magnetic hot spot and a clockwise current loop can be observed in Fig.2(g). M_2 is defined as a dark magnetic mode. Mode M_3 is a quadrupole-quadruple mode, which has a larger net dipole moment and a wider linewidth, so mode M_3 is a bright mode. Fig.2(i) shows that the mode M_3 has a magnetic hot spot and a counterclockwise current loop, so m_3 is a magnetic mode. According to the formation theory of Fano resonance, dip m_2 is generated by the destructive interference between dark magnetic mode M_2 and bright magnetic mode M_3. A magnetic hot spot and a counterclockwise current loop are observed in Fig.2(h), so dip m_2 is a magnetic Fano resonance. However, dip m_1 is not Fano resonance because both M_1 and M_2 are dark modes and the coupling distance is large.

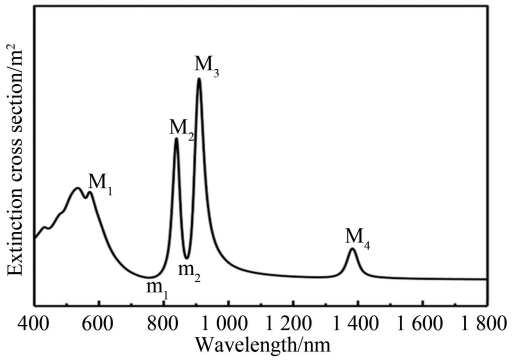

(a) The extinction cross section of the SSR-DSD nanostructure

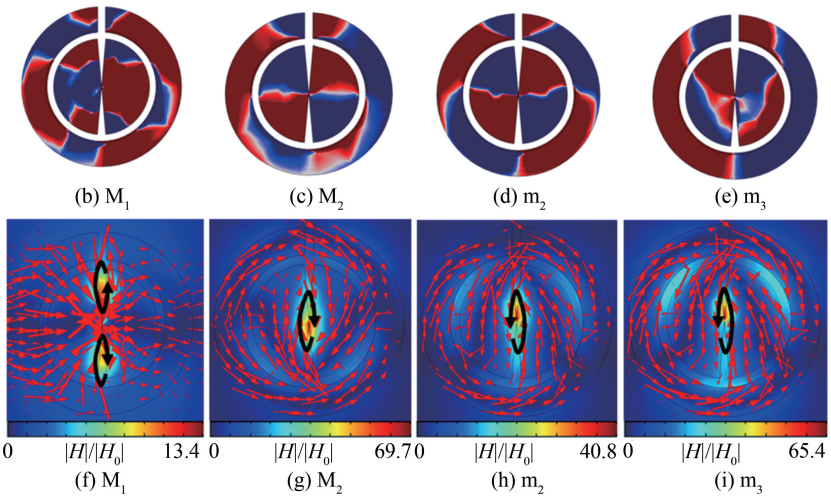

(b) M_1 (c) M_2 (d) m_2 (e) m_3

(f) M_1 (g) M_2 (h) m_2 (i) m_3

Fig.2 The extinction cross section, the charge distribution, the current density and magnetic field enhancement distribution of the SSR-DSD structure

2.2 Breaking the symmetry of the structure

High order magnetic mode and new magnetic Fano resonance can be achieved by further breaking the structure symmetry. Fig.3(a) shows the extinction cross section of the nanostructure when the double-split disk, the cavity and the gap of the single-split ring offset together along the negative x-axis by 4.5 nm, 9 nm, 13.5 nm and 18 nm. The offset produce a phase delay, so a new resonance peak M_5 appears at the wavelength of 690 nm. As shown in Fig.3(b), M_5 is a quadrupole-quadrupole mode, which has a large net dipole moment. Mode M_5 has four magnetic hot spots and adjacent current loops are in opposite directions, so M_5 is defined as a magnetic mode. As the offset increases, the intensity of mode M_5 increases, but the intensity of mode M_2 decreases, because the symmetry of the structure is further broken and the charge distribution is more uneven. As shown in Fig.3(c) and (e), the magnetic field of M_5 is mainly distributed in the cavity of the structure, while the magnetic field of M_2 is mainly in the center of the double-split disk, so magnetic field enhancement is transferred from the double-split disk to the cavity of the structure.

Dip m_3 is generated by the interference between dark magnetic mode M_1 and bright magnetic mode M_5. As shown in Fig.3(d), dip m_3 has four current loops and adjacent loops are in opposite directions, so it is a magnetic Fano resonance. With the increases of the offset, a new resonance peak M_6 appears at the

long wavelength of 1 180 nm. In Fig.3(f) and (g), the magnetic field of M_4 is mainly distributed in the center of the double-split disk, while the magnetic field of M_6 is mainly distributed on both sides of the cavity, so magneticfield enhancement is transferred from the cavity to the double-split disk. There are two magnetic Fano dip (m_2 and m_3) in Fig.3(a), which is called double magnetic Fano resonances.

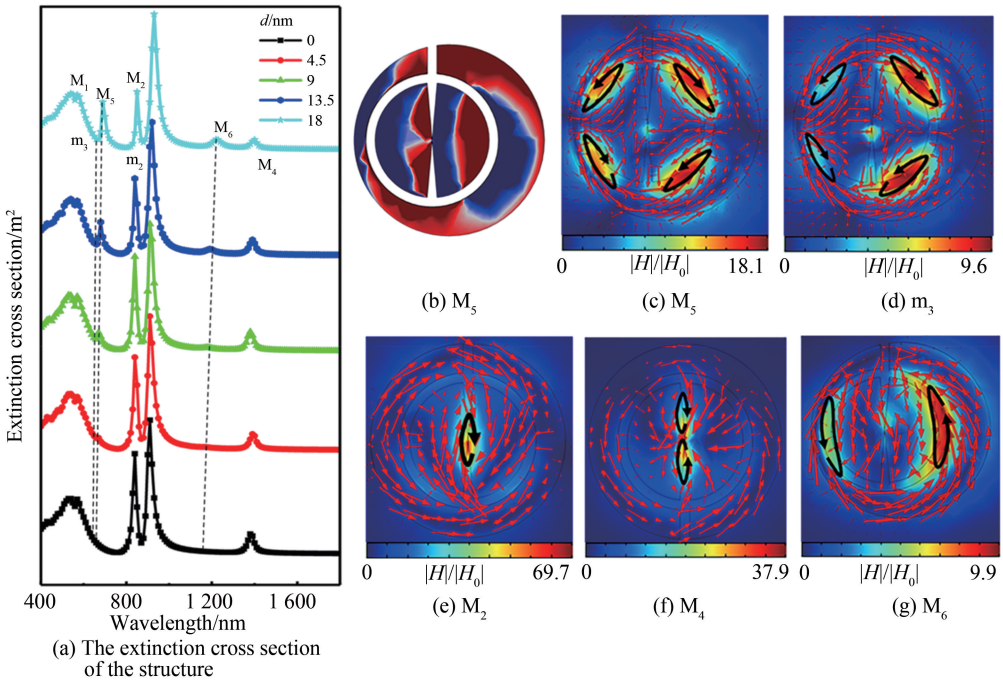

Fig.3 The extinction cross section, the charge distribution, the current density and magnetic field enhancement distribution of the structure when offset d

2.3 Increasing the gap width of the single-split ring

Surface plasmon resonance is very sensitive to structure parameters, so we further increase the gap width of the single-split ring on the basis of the nanostructure with $d=18$ nm. As shown in Fig.4 (a), at the long wavelength, mode M_6 and M_4 are enhanced with the increase of the gap width of the single-split ring. M_4 is a dipole-dipole mode and has a large net dipole moment, which is a bright mode. Fig.4(c) shows that M_6 is a quadrupole-dipole mode. Dip m_4 is generated by the interference between the bright magnetic mode M_4 and the dark magnetic mode M_6, which has a counterclockwise current loop on the left of the cavity, so dip m_4 is a magnetic Fano resonance. Dips m_2, m_3, and m_4 can be defined as the triple magnetic Fano resonances.

In the case, the split ring is similar to capacitor and inductor in series. The resonance frequency formula can be expressed as

$$f=\frac{1}{\sqrt{LC}} \tag{1}$$

where f is the resonance frequency, L represents the inductance and C represents the capacitance. C is the capacitance between the two arms of the single-split ring, which is inversely proportional to the distance between the arms. With the increase of the distance between the arms, the capacitance decreases, and the frequency increases, which result in a significant blue shift of magnetic modes M_6 and M_4. It can also be understand that increasing the gap width of the single-split ring, the distribution distance of the charge on the single-split ring becomes shorter, which leads to the enhancement of restoring force and the blue shift of modes M_4, M_6 and dip m_4. Figs.4(e) and (f) show the dependence of the resonance wavelength and intensity on the gap width of the single-split ring.

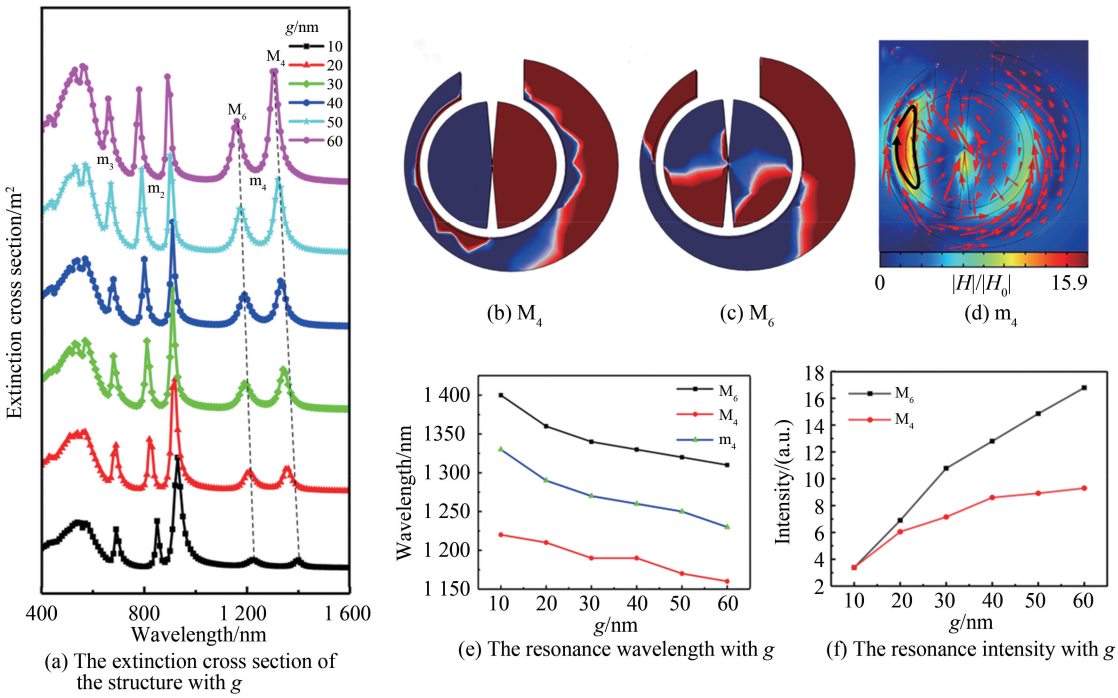

Fig.4 The extinction cross section, the charge distributions, the current density and magnetic field enhancement distribution of the structure when different g

In order to explore the sensitivity of Fano resonance to the refractive index of the external environment, we give the extinction spectra with different refractive indexes 1.00, 1.05, 1.10, 1.15 and 1.20. As shown in Fig.5(a)～(b), peaks M_4, M_6 and dip m_4 all have a significant red shift with the increase of the refractive index. In order to better describe the potential applications of the structure in sensing, the FOM is studied, which is an important parameter to evaluate sensing performance. FOM is defined as

$$\mathrm{FOM}=\frac{S}{\mathrm{FWHM}} \tag{2}$$

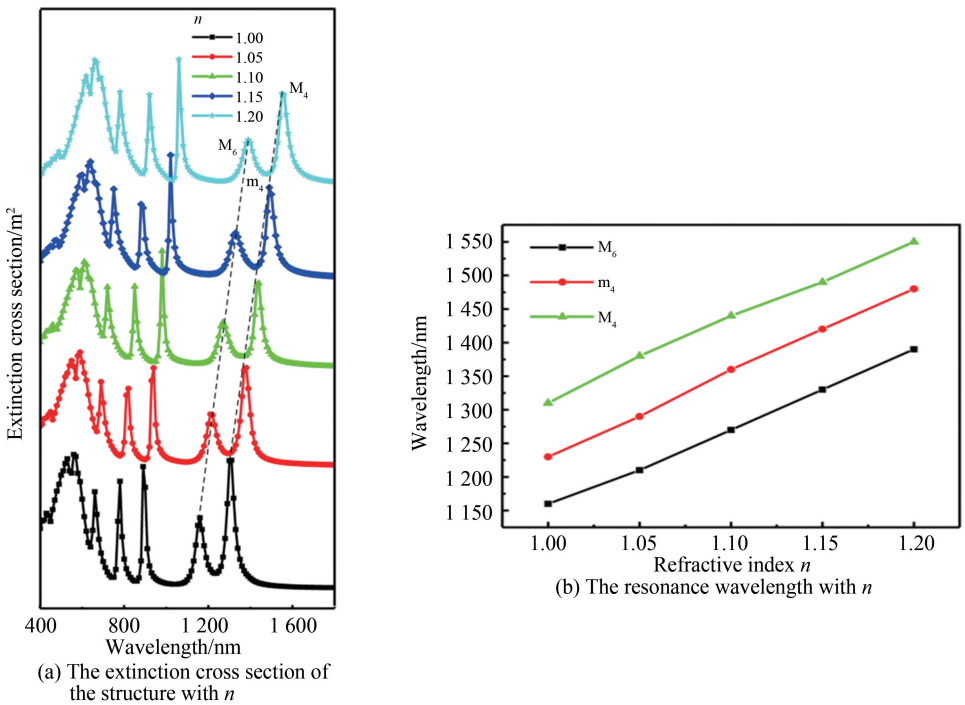

Fig.5 The extinction cross section and the resonance wavelength of the structure with different n

where S is the refractive index sensitivity, and FWHM is the full width at half maximum of the resonance peak. The refractive index sensitivity S can be expressed as

$$S = \frac{\delta\lambda}{\delta n} \tag{3}$$

where $\delta\lambda$ represents the displacement of the resonance peak, and δn is the change of the refractive index. In our strucure, the sensitivity of dip m4 is 1 400 nm/RIU and the maximum FOM value is 29.43, which is on a fairly ideal level. Therefore, the structure has potential application in sensor.

2.4 Increasing the upper split angle of the double-split disk

Here, we further study the extinction characteristics of the structure with offset $d = 18$ nm by increasing the upper split angle of the double-split disk. As shown in Fig.6(a), a new resonance peak M_7 appears at the short wavelength of the spectrum. In Fig.6(b), M_7 is a quadrupole-octupole mode, which has a large net dipole moment. Mode M_7 has three magnetic hot spots and three current loops, but the central current loop is opposite to the inter-cavity current loops. Dip m_5 is generated by the interference between the bright magnetic mode M_7 and the dark magnetic mode M_1. Dip m_5 has two magnetic hot spots and two current loops in opposite directions, so m_5 is a magnetic Fano resonance mode. Dips m_2, m_3 and m_5 are called triple magnetic Fano resonances.

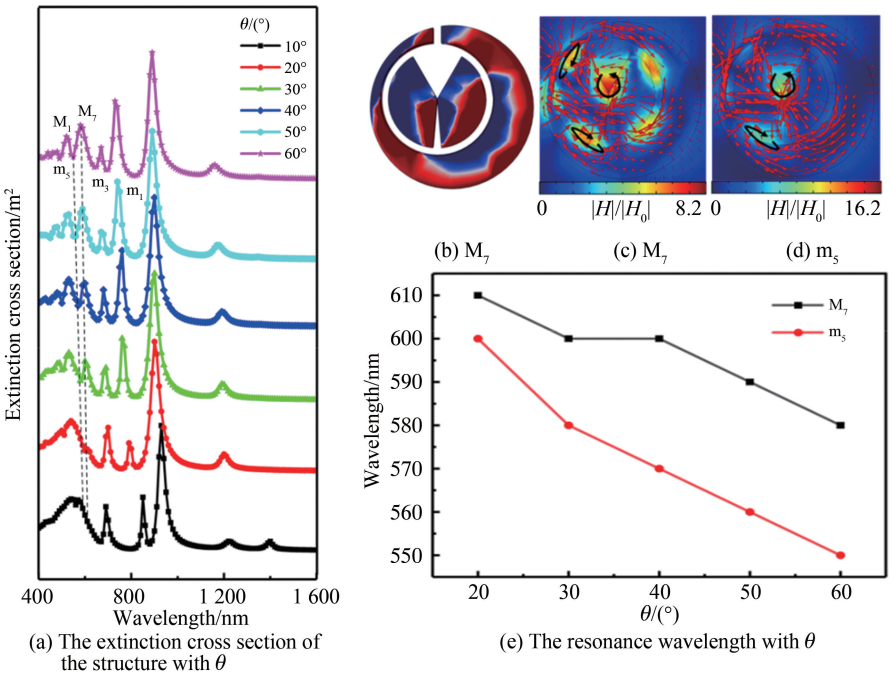

Fig.6 The extinction cross section, the charge distribution, the current density and magnetic field enhancement distributions, the resonance wavelength with different θ

In Fig.6(e), it can be clearly observed that the variation of resonance wavelengths of mode M_7 and m_5 when the upper split angle of the double-split disk increases. By comparing the phenomena generated by the regulation of the single-split ring and the double-split disk, it can be concluded that the regulation of the single-split ring mainly affects the magnetic modes and magnetic Fano resonance in the near-infrared region, while the regulation of the double-split disk mainly affects that of the visible region. Therefore, magnetic mode and magnetic Fano resonance can be obtained in different wavebands according to actual needs. This characteristic of the structure makes it have potential applications in multiple magnetic Fano switch.

3 Conclusion

The nanostructure consisting of a Single-Split Ring and a Double-Split Disk (SSR-DSD) is designed and studied. When the incident light is normal to the structure surface, magnetic Fano resonance can be generated by the interference between a bright magnetic mode and a dark magnetic mode. High order

magnetic modes and multiple magnetic Fano resonances can be generated when the double-split disk, the cavity and the gap of the single-split ring offset together along the negative x-axis. On the basis of this structure, magnetic modes and magnetic Fano resonance can also be generated in the near-infrared and visible wavelengths by modulating the gap width of the single-split ring and the upper split angle of the double-split disk. In addition, the maximum sensitivity of the new resonance mode is 1 400 nm/RIU and the maximum FOM is 29.43. The magnetic field enhancement of the structure has also reached 69.7. These excellent optical properties make the SSR-DSD nanostructure have potential applications in ultra-sensitive biosensor, multi-control magnetic Fano switch.

References

[1] BARNES W L, DEREUX A, EBBESEN T W. Surface plasmon subwavelength optics[J]. *Nature*, 2003, **424**(6950): 824-830.

[2] LI Gang, GUAN Wen-jun, ZHANG Yan-jun, *et al*. Polarization-controlled optical switch basedon surface plasmon[J]. *Acta Photonica Sinica*, 2020, **49**(3): 0326001.

[3] YAN Yun-fei, ZHANG Guan-mao, QIAO Li-tao, *et al*. Designonthe convex ring MIM structure filter based on surface plasmon polaritons[J]. *Acta Photonica Sinica*, 2019, **48**(2): 0223002.

[4] LANCE K K, CORONADO E, ZHAO L L, *et al*. The optical properties of metal nanoparticles: the influence of size, shape, and dielectric environment[J]. *Journal of Physical Chemistry B*, 2003, 107(3): 668-677.

[5] MOCK J J, SMITH D R, SCHULTZ S. Local refractive index dependence of plasmon resonance spectra from individual nanoparticles[J]. *Nano Letters*, 2003, **3**(4): 485-491.

[6] PAYNE E K, SHUFORD K L, PARK S, *et al*. Multipole plasmon resonances in gold nanorods[J].*Journal of Physical Chemistry B*, 2006, **110**(5): 2150-2154.

[7] MA Guang-hui, ZHANG Jia-bin, WANG Xiao-yi, *et al*. Gold localized surface plasmon enhanced luminescence characteristics of gallium arsenide[J]. *Acta Photonica Sinica*, 2019, **48**(5): 0526002.

[8] ZARRABIA F B, KUHESTANIB H, RAHIMIC M, *et al*. Plasmonic cross-junction ring antenna implementation for field Enhancement[J]. *Optik*, 2015, **126**(21): 3129-3131.

[9] HE Bing-qian, LI Yong-hong, CAO Ya-nan, *et al*. Tunable fano resonance basedon metal square corestructure embedded in MIM resonator[J]. *Acta Photonica Sinica*, 2018, **47**(11): 174-181.

[10] MAYER K M, HAFNER J H. Localized surface plasmon resonance sensors[J]. *Chemical Reviews*, 2011, **111**(6): 3828-3857.

[11] SOW I, GRAND, LEVI G, *et al*. Revisiting surface-enhanced raman scattering on realistic lithographic gold nanostripes [J]. *Journal of Physical Chemistry C*, 2013, **117**(48): 25650-25658.

[12] DONG Jun, QU Shi-xian, ZHENG Hai-rong, *et al*. Simultaneous SEF and SERRS from silver fractal-like nanostructure[J]. *Sensors and Actuators*, 2014, **B191**(Feb.): 595-599.

[13] HU Sen, LIU Dan, YANG He-lin. Electromagnetic induced transparency based on all-dielectric metasurface[J]. *Acta Photonica Sinica*, 2018, **047**(11):211-219.

[14] LIM Wen-xiang, SINGH Ran-jan. Universal behaviour of high-Q Fano resonances in metamaterials: terahertz to near-infrared regime[J]. *Nano Convergence*, 2018, **5**(1): 0-6.

[15] MIROSHNICHENKO A E, KIVSHAR Y S. Engineering Fano resonances in discrete arrays[J]. *Physical Review E Statistical Nonlinear & Soft Matter Physics*, 2005, **72**(2): 056611.

[16] ZHU Zhi-qiang, SU Yuan-yuan, LI Jiang, *et al*. Highly sensitive electrochemical sensor for mercury(II) ions by using a mercury-specific oligonucleotide probe and gold nanoparticle-based amplification[J]. *Analytical Chemistry*, 2009, **81**(18): 7660-7666.

[17] KHAN A D, KHAN S D, KHAN R U, *et al*. Excitation of multiple fano-like resonances induced by higher order plasmon modes in three-layered bimetallic nanoshell dimer[J]. *Plasmonics*, 2014, **9**(2): 461-475.

[18] KHAN A D, KHAN S D, KHAN R U, *et al*. Generation of multiple fano resonances in plasmonic split nanoring dimer [J]. *Plasmonics*, 2014, **9**(5): 1091-1102.

[19] LIU Shao-ding, YANG Zhi, LIU Rui-ping, *et al*. Multiple fano resonances in plasmonic heptamer clusters composed of split nanorings[J]. *Acs Nano*, 2012, **6**(7): 6260-6271.

[20] LI Jing, ZHANG Yi, JIA Tian-qing, *et al*. High tunability multipolar fano resonances in dual-ring/disk cavities[J]. *Plasmonics*, 2014, **9**(6): 1251-1256.

[21] SMITH D R, PADILLA W J, VIER D C, *et al*. Composite medium with simultaneously negative permeability and permittivity[J]. *Physical Review Letters*, 2000, **84**(18): 4184-4187.

[22] ZHANG Hao, TONG Yuan-wei. Tunable pass-band filter based on one dimensional split ring resonant structure[J]. *Acta Photonica Sinica*, 2018, **47**(7): 190-196.

[23] GRIGORENKO A N, GEIM A K, GLESSON H F, *et al*. Nanofabricated media with negative permeability at visible frequencies[J]. *Nature*, 2005, **438**(7066): 335-338.

[24] WANG J, FAN C, HE J, *et al*. Double Fano resonances due to interplay of electric and magnetic plasmon modes in planar plasmonic structure with high sensing sensitivity[J]. *Optics Express*, 2013, **21**(2): 2236.
[25] LIU N, MUKHERJEE S, BAO K, *et al*. Magnetic plasmon formation and propagation in artificial aromatic molecules [J]. *Nano Letters*, 2012, **12**(1): 364-369.
[26] LIU N, MUKHERJEE S, BAO K, *et al*. Manipulating magnetic plasmon propagation in metallic nanocluster networks [J]. *Acs Nano*, 2012, **6**(6): 5482-5488.
[27] ZHOU J, KOSCHNY T, KAFESAKI M, *et al*. Saturation of the magnetic response of split-ring resonators at optical frequencies[J]. *Physical Review Letters*, 2005, **95**(22): 223902.
[28] SHAFIEI F, MONTICONE F, LE K Q, *et al*. A subwavelength plasmonic metamolecule exhibiting magnetic-based optical Fano resonance[J].*Nature Nanotechnology*, 2013, **8**(2): 95-99.
[29] ZHAO Kai-jun, HUO Yi-ping, LIU Ting-zhuo *et al*. Manipulation of magnetic fano resonances in double split-hole disk [J]. *Plasmonics*, 2016, **11**(1): 269-275
[30] NAZIR A, PANSRO S, PROIETTI ZACCARIA R, *et al*. Fano coil-type resonance for magnetic hot-spot generation [J]. *Nano Letters*, 2014, **14**(6): 3166-3171.
[31] SHOROKHOV A S, MELIK-GAYKAZYAN E V, SMIRNOVA D A, *et al*. Multifold enhancement of third-harmonic generation in dielectric nanoparticles driven by magnetic fano resonances[J]. *Nano Letters*, 2016, **16**: 4857-4861.
[32] CHERQUI C, WU Yue-ying, LI Guo-liang, *et al*. STEM/EELS imaging of magnetic hybridization in symmetric and symmetry-broken plasmon oligomer dimers and all-magnetic fano interference[J]. *Nano Letters*, 2016, **16**: 6668-6676.
[33] PANARO S, NAZIR A.,PROIETTI Z R *et al*. Plasmonic moon: a fano-like approach for squeezing the magnetic field in the infrared [J]. *Nano Letters*, 2015, **15**: 6128-6134.
[34] BAO Yan-jun, HU Zhi-jian,LI Zi-wei, *et al*. Magnetic plasmonic Fano resonance at optical frequency[J]. *Small*, 2015, **11**(18): 2177-2181.
[35] SHEIKHOLESLAMI S N, GARCIA-ETXARRI A, DIONNE J A. Controlling the interplay of electric and magnetic modes via Fano-like plasmon resonances[J]. *Nano Letters*, 2011, **11**(9): 3927-3934.
[36] NEMATI A, WANG Qian, HONG Ming-hui, *et al*. Tunable and reconfigurable metasurfaces and metadevices[J]. *Opto-Electronic Advances*, 2018, **1**(5): 180009.
[37] GUO Shu-ting, CHEN Min-cheng, ZHANG Yu-hong, *et al*. Observation of Fano resonance in one whispering-gallery-mode microresonator[J]. *Acta Photonica Sinica*, 2019, **48**(11): 1148021.
[38] LIU Zheng-qi, LIU Gui-qiang, LIU Xiao-shan, *et al*. Plasmonic sensors with an ultra-high figure of merit [J]. *Nanotechnology*, 2019, **31**(11): 115208.
[39] LIU Zheng-qi, YU Mei-dong, HUANG Shan, *et al*. Enhancing refractive index sensing capability with hybrid plasmonic-photonic absorbers[J]. *Journal of Materials Chemistry C*, 2015, **3**(17): 4222-4226.
[40] JOHNSON P B, CHRISTY R W. Optical constants of the noble metals[J]. *Physical Review B* (*Solid State*), 1972, **6** (12): 4370-4379.
[41] JIN J M. The finite element method in electromagnetics[M]. John Wiley & Sons, 2002.
[42] LI Yuan, HUO Yi-ping, ZHANG Ying, *et al*. Generation and manipulation of multiple magnetic Fano resonances in split ring-perfect ring nanostructure[J]. *Plasmonics*, 2017, **12**: 1613-1619.